LA-UR-21-20333

Approved for public release; distribution is unlimited.

Title: Initial conditions for simulations of beam physics in linear induction accelerators

Author(s): Ekdahl, Carl August Jr.

Intended for: Report

Issued: 2021-01-14

Initial Conditions for Simulations of Beam Physics in Linear Induction Accelerators

Carl Ekdahl

I. Introduction

FLASH radiography of hydrodynamic experiments driven by high explosives is a well-known diagnostic technique in use at many laboratories [1, 2]. At Los Alamos, the Dual-Axis Radiographic Hydrodynamic Test (DARHT) facility two linear induction electron accelerators (LIAs) make the bremsstrahlung radiographic source spots for point projection radiographs from orthogonal views. A new LIA, called Scorpius, is presently under development to advance this technology.

To better understand electron-beam physics in these LIAs, numerical simulations are frequently performed with the objective of improving the radiography. At Los Alamos we frequently use the TRAK ray-trace and LSP particle-in-cell (PIC) codes to simulate the injector, and the XTR and LAMDA envelope/centroid codes along with LSP to simulate transport of the accelerated beam through the LIAs. The LIA simulations need the injected beam parameters as initial conditions for calculating beam transport and stability. The determination of these initial conditions is the topic of this note.

II. Required Initial Conditions

Beam physics at DARHT is simulated using the beam envelope equation [3, 4, 5, 6, 7, 8, 9], the equation of motion of the beam centroid [5, 8, 10, 11], and PIC codes [12, 13]. Integration of the second order differential equation for the beam envelope requires the initial envelope radius and convergence, as well as the beam energy, current, and normalized emittance, which is presumed invariant [3, 4]. (The emittance in our codes is the 4-rms Lapostolle value that describes an equivalent Kapchinsky-Vladimirsky (K-V) distribution [14].)

PIC code simulations of DARHT and Scorpius using a slice model [12] frequently launch the beam as a rigidly-rotating distribution, as expected for transport of a beam perfectly matched to externals focusing forces. Evolution of the initial distribution due to beam mismatch then appears as emittance growth as the beam propagates through the LIA [13]. The beam parameters required to establish the initial rigid-rotor distribution are the same as those needed for the envelope codes; i.e., envelope radius, envelope convergence, normalized emittance, energy, and current.

Since our foremost envelope code, XTR, has no provision for external electric fields other that due to cell gaps, we choose the location of the hand-off from diode simulations to be far enough into the anode beam pipe that the applied diode potential has decayed to less than the expected beam space charge depression for a uniform current distribution;

$$\delta\varphi_{sc} = 30\left(I_b / \beta\right)\left[1 + 2\ln\left(R_W / R_{env}\right)\right] \tag{1}$$

where I_b is the beam current, $\beta = v / c$, and R_{env} and R_W are the beam-envelope and beam-pipe radii.

III. Injected Beam Parameters

In our accelerators the electron beam is produced in a diode having either a cold, explosive-emission cathode (DARHT-I) or a hot, dispenser cathode (DARHT-II and Scorpius). Beam parameters at the exit of the diode are the initial conditions for simulations of the LIA, and have been measured (DARHT-I), or calculated with TRAK (DARHT-II and Scorpius).

Injected beam parameters on DARHT-I have been carefully measured with beam positon monitors (BPMs), dipole-magnet spectrometers, and focusing solenoid scans. BPM measurements provide required current, spectrometer measurements provide beam energy, and analysis of solenoid scans provide envelope radius, convergence, and emittance. Where such measurements are not feasible (DARHT-II and Scorpius design) we have relied on simulations with TRAK, which have been corroborated with PIC code simulations.

In addition to beam energy and current, TRAK returns three rms beam parameters calculated from current-weighted second moments of the distribution, and two estimates of envelops parameters based on the trajectory of the outermost particle. These are listed in Table I.

Table I. TRAK output

Parameter	Symbol	Units
Kinetic Energy	KE	eV
Current	I_b	A
RMS Radius	$\left\langle r^2 \right\rangle^{1/2}$	m
RMS Angle	$\left\langle r'^2 \right\rangle^{1/2}$	radian
RMS Emittance	ε	m-radian
Envelope Radius	R_{env}	m
Envelope Convergence	R'_{env}	radian

Here, brackets indicate moments over the beam distribution, prime indicates derivatives with respect to axial distance; e.g., $r' = dr/dz$.

The emittance calculated by TRAK is the 4-rms Lapostolle value [15]

$$\varepsilon = 2\left(\langle r^2\rangle\langle r'^2\rangle - \langle rr'\rangle^2\right)^{1/2} \quad (2)$$

from which we derive the required normalized emittance; $\varepsilon_n = \beta\gamma\varepsilon$, where $\beta = v/c$ and $\gamma = 1 + KE/m_e c^2$.

From the TRAK output, we get the initial conditions needed for our envelope and PIC-Slice codes. The envelope equations in our codes are based on a derivation that describes the self-similar variation of the rms radius of an arbitrary radial current distribution of an axisymmetric beam as it is transported and accelerated [4]. This second-order differential equation needs the initial rms radius, R_{rms} , and its convergence, R'_{rms} . The convergence based on moments is not given by TRAK, but it can be derived based on its relation to the cross correlation term in the emittance. That is

$$\frac{d}{dz}R_{rms}^2 = \frac{d}{dz}\langle r^2\rangle = 2\langle rr'\rangle \quad (3)$$

or,

$$R_{rms}R'_{rms} = \langle rr'\rangle \quad (4)$$

It follows from Eq. (2) that one has

$$R'_{env} = \left[\langle r'^2\rangle - (\varepsilon/2)^2 / \langle r^2\rangle\right]^{1/2} \quad (5)$$

where all quantities on the right are directly available from TRAK output.

The envelope radius used in our codes is self-consistently defined as the edge radius of an equivalent uniform current distribution [3]; that is, $R_{env} = R_{rms}\sqrt{2}$ .It follows that the same factor is applicable to beam convergence, $R'_{env} = R'_{rms}\sqrt{2}$ .These are the initial values used in XTR, and LAMDA. TRAK output also includes estimates of R_{env} and R'_{env} based on the outermost ray of the distribution. These are often compared with the values derived from moments as a check of consistency with the ideal uniform distribution, and. are usually within a few percent of the derived values.

IV. EXAMPLES

To illustrate, we present two examples of LIA simulations handed off from TRAK simulations of a diode; the first for DARHT-II, and the second for a recent design of Scorpius. Fig.1 shows a TRAK simulation of the DARHT-II diode indicating the location at 79.38 cm from the cathode where parameters are handed off to other codes for further calculations. Using initial conditions derived from TRAK, beam transport through the LIA was simulated by XTR (Fig. 2) and LSP (Fig. 3, which also shows the calculated emittance). The same sequence of illustrations are shown for a 102-cell solid-state powered design of Scorpius in Fig. 4, Fig. 5, and Fig. 6. The initial conditions used for the envelope and PIC simulations are listed in Table II.

Table II: Initial conditions for LIA simulations.

Parameter	Units	DARHT-II	Scorpius
KE	MeV	2.2	2.0
I_b	kA	1.68	1.4452
R_{env}	cm	8.83	5.011
R'_{env}	m-radian	26.3	-35.24
ε_n	cm-radian	0.0206	0.02036

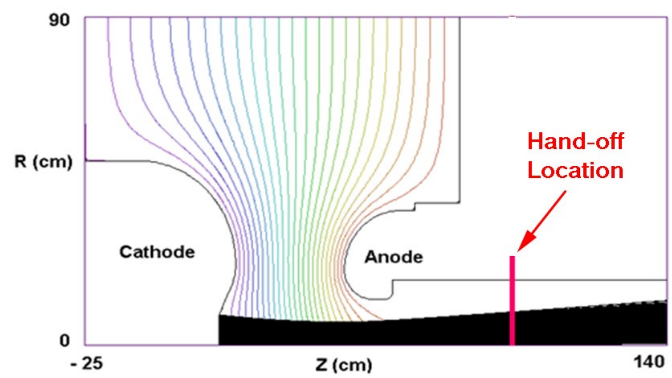

Fig. 1: TRAK simulation of electron beam production in the DARHT-II diode. The handoff to other codes for simulations of beam dynamics through the LIA is at the indicated position 79.38 cm downstream of the cathode, where the electric potential applied to the AK gap is attenuated to less than the beam space-charge potential.

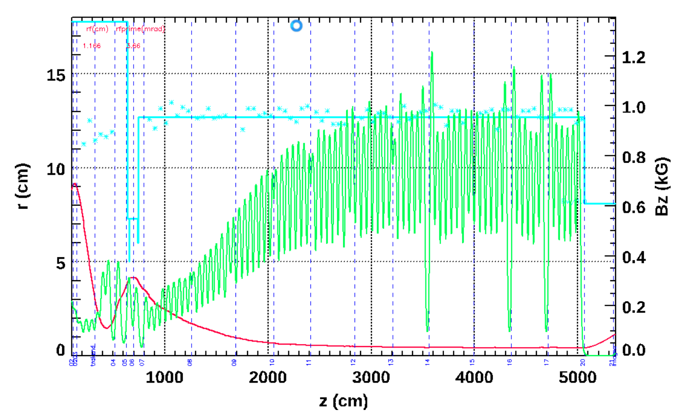

Fig.2: XTR envelope code simulation of beam transport and acceleration through the DARHT-II LIA. Red Curve: Beam envelope radius (left scale). Green Curve: Solenoidal magnetic field on axis (right scale).Solid Cyan Lines :Beam pipe and apertures inner radii(left scale). Cyan Asterisks: Relative gap potentials.

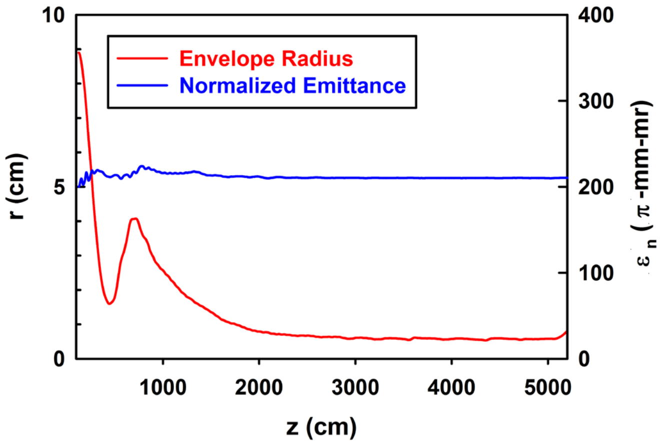

Fig. 3: LSP slice PIC code simulation of beam transport and acceleration through the DARHT-II LIA with the tune shown in Fig.2. Red Curve: Beam envelope radius (left scale). Blue Curve: Normalized 4-rms emittance (right scale)

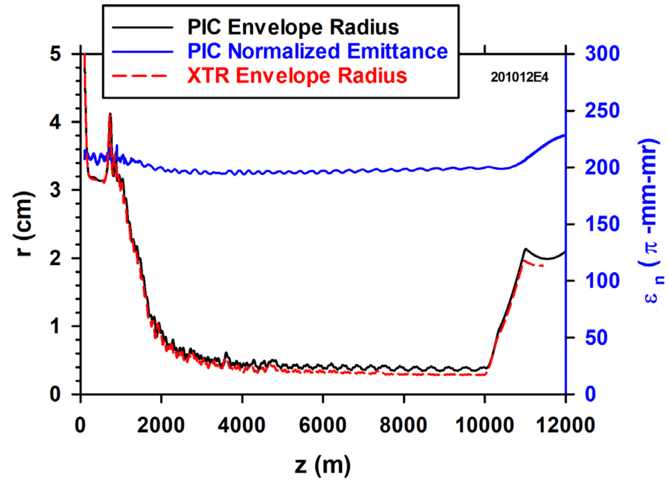

Fig. 6: LSP slice PIC code simulation of beam transport and acceleration through the 102-cell Scorpius LIA with the tune shown in Fig. 5Fig.2. Black Curve: Beam envelope radius simulated by the LSP PIC code (left scale).Dashed Red Curve: Beam envelope radius simulated by the XTR envelope code (left scale). Blue Curve: Normalized 4-rms emittance (right scale).

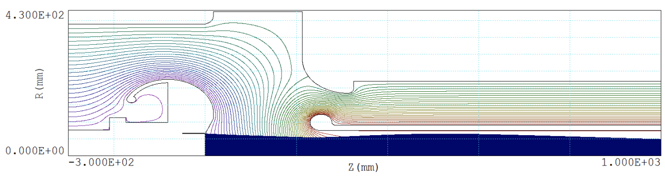

Fig. 4: TRAK simulation of electron beam production in the Scorpius diode. The handoff to other codes for simulations of beam dynamics through the LIA is at a position at the right boundary 100 cm downstream of the cathode, where the electric potential applied to the AK gap is attenuated to less than the beam space-charge potential.

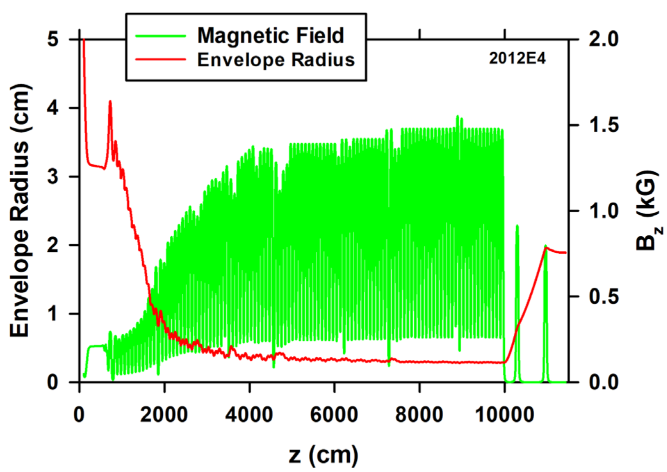

Fig. 5: XTR envelope code simulation of beam transport and acceleration through the 102-cell Scorpius LIA. Red Curve: Beam envelope radius (left scale). Green Curve: Solenoidal magnetic field on axis (right scale).

Neither the DARHT-II nor the Scorpius tunes used for these simulations resulted in appreciable betatron oscillations of the envelope, or emittance growth. The DARHT-II tune was in use on the LIA from 2013 through 2020, which included several hydrotests with radiography.

V. Conclusion

Although TRAK simulations of the injectors for our LIAs do not directly provide the beam envelope convergence required by the envelope and PIC codes used for simulating transport through the LIA, there is enough information to derive it.

Acknowledgment

The author thanks his colleagues at DARHT and the Scorpius project, and to Stanley Humphries (the author of TRAK), for many stimulating discussions about beamphysics.

References

[1] C. Ekdahl, "Modern electron acccelerators for radiography," *IEEE Trans. Plasma Sci.,* vol. 30, no. 1, pp. 254-261, 2002.

[2] K. Peach and C. Ekdahl, "Particle radiography," *Rev. Acc. Sci. Tech.,* vol. 6, pp. 117 - 142, 2013.

[3] F. Sacherer, "RMS envelope equations with space charge," *IEEE Trans. Nucl. Sci.,* vol. 18, pp. 1105 - 1107, 1971.

[4] E. P. Lee and R. K. Cooper, "General envelope equation for cylindrically symmetric charged-particle beams," *Part. Accel.,* vol. 7, pp. 83-95, 1976.

[5] J. D. Lawson, The physics of charged particle beams, Oxford: Clarendon, 1977.

[6] C. Ekdahl, "Modeling ion-focused transport of electron beams with simple beam-envelope simulations," Sandia National Laboratories Report SAND86-0544, 1986.

[7] S. Humphries, Charged Particle Beams, New York: Wiley, 1990.

[8] P. Allison, "Beam dynamics equations for XTR," Los Alamos National Laboratory report, LA-UR-01-6585, 2001.

[9] T. Genoni, T. Hughes and C. Thoma, "Improved envelope and centroid equations for high current beams," in *AIP Conf. Proc.*, 2002.

[10] C. Ekdahl and et. al, "Electron beam dynamics in the long-pulse, high-current DARHT-II linear induction accelerator," in *Part. Accel. Conf.*, Vancouver, BC, CA, 2009.

[11] C. Ekdahl, "Tuning the DARHT long-pulse linear induction accelerator," *IEEE Trans. Plasma Sci.,* vol. 41, pp. 2774 - 2780, 2013.

[12] C. Thoma and T. P. Hughes, "A beam-slice algorithm for transport of the DARHT-2 accelerator," in *Part. Acc. Conf.*, 2007.

[13] C. Ekdahl and et al., "Emittance growth in the DARHT-II linear induction accelerator," *IEEE Trans. Plasma Sci.,* vol. 45, no. 11, pp. 2962 - 2973, Nov 2017.

[14] P. M. Lapostolle, "Possible emittance increase through filamentation due to space charge in continuous beams," *IEEE Trans. Nucl. Sci.,* vol. 18, pp. 1101 - 1104, 1971.

[15] S. Humphries, "Tutorial: Emittance calculations for circular beams," [Online]. Available: http://www.fieldp.com/library.html#tutorial. [Accessed December 2020].